J. Fluid Mech. (1982), *vol.* 118, *pp.* 27–40
Printed in Great Britain

On the nature of the dynamic contact angle: an experimental study

By CLIFTON G. NGAN AND ELIZABETH B. DUSSAN V.

Department of Chemical Engineering, University of Pennsylvania, Philadelphia, Pennsylvania, U.S.A.

(Received 27 May 1981 and in revised form 3 August 1981)

The dynamic contact angle formed when silicone oil displaces air from the surface of glass has been measured. Even though the glass was neither treated in any special way nor cleaned by an elaborate technique, the standard deviation associated with our measurements was approximately 1·5°. A sequence of experiments revealed that the dynamic contact angle depends on both the speed at which the oil spreads across the glass and the size of the characteristic length scale associated with the device within which it is measured. It is shown that the latter implies directly that: (i) the *measured* and the *actual* contact angles are not the same; (ii) the usual hydrodynamic model for fluids is inadequate when a moving contact line is present. These conclusions are consistent with recent theoretical studies.

1. Introduction

Whenever a liquid spreads over a solid surface, a moving contact line is formed. Investigators in various fields are interested in discerning which factors play a role in determining the rate at which this line moves, and in understanding how these factors interact. Areas where the rate of spreading can be important are agrichemicals, coating and adhesives, lubrication, oil recovery and immiscible fluid displacement through porous media, as well as nucleate boiling and dropwise condensation.

To date, very little has been discovered about the mechanism by which a liquid wets a solid. While various experimental techniques have been used, they have usually lacked the resolution necessary to extract information that might give insight into this process. Over the years, the microscope has emerged as the principal tool for investigating the wettability of solids, with interferometers, ellipsometers, and other instruments playing relatively minor roles. Regardless of the type of instrument used, the predominant quantity which has been reported for experiments under both static and dynamic conditions is the *contact angle* (see figure 1).

While little is known from a molecular point of view about the nature of the dynamic contact angle, its role in fluid mechanics, be it static or dynamic, is quite clear. It serves as a boundary condition for the nonlinear partial differential equation which describes the behaviour of the gas–liquid interface.†

Although it would be useful to have a theoretically derived expression for the contact angle, it is by no means necessary. As with other quantities that appear in

† All our comments are valid for material systems consisting of two immiscible fluids and a solid. For convenience, we refer to the two immiscible fluids as a gas and a liquid.

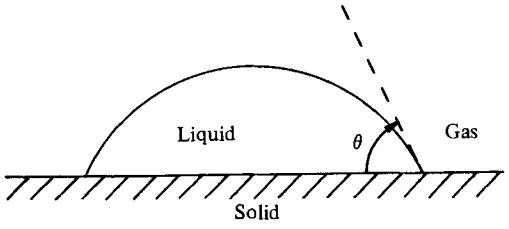

FIGURE 1. The contact angle θ is formed between the plane tangent to the fluid–fluid interface at the contact line, and the plane tangent to the solid surface.

the conservation equations in continuum mechanics, e.g. the stress tensor, and the energy- and mass-flux vectors, precise expressions are almost always determined experimentally.

The most popular apparatus for measuring the behaviour of the contact angle is the capillary, a glass tube with an inner diameter of 0·2 cm or less. However, when the liquid or solid is not transparent, other configurations must be used. Some examples consist of a drop spreading on a horizontal surface (Schonhorn, Frisch & Kwei 1966), or tapes and wires entering (or leaving) a bath of liquid (Blake & Ruschak 1979; Schwartz & Tejada 1972).

Typically, the contact angle is measured by one of two methods. The most direct approach, although probably the least accurate, uses a protractor. The protractor can either be inscribed on the eyepiece of a microscope with the measurement of the contact angle accomplished by direct observation, or it be used on an enlargement of a photograph of the gas–liquid interface in the vicinity of the contact line. The second technique for measuring the contact angle can only be used when the motion of the fluid is relatively slow, i.e. for small capillary numbers (refer to § 4 for definition). This method takes advantage of the fact that the shape of the gas–liquid interface must be a member of an already identified family. For example, the shape of the gas–liquid interface in a narrow capillary is that of a segment of a sphere. The contact angle can then be calculated upon measuring a specific characteristic of the interface. Thus, by measuring h/a, the ratio of the apex height – the distance between the plane containing the contact line and the apex of the interface – to the radius of the capillary, the contact angle θ_{app}† can be determined from the following relationship:

$$\cos\theta_{\text{app}} = \frac{-2h/a}{1+(h/a)^2}. \tag{1}$$

Hoffman (1975) performed a series of experiments in which various non-polar liquids were forced to displace air through glass capillaries of approximately 0·2 cm inner diameter. Both treated and cleaned surfaces were used so that the effect of the static contact angle could be explored. He found that all of his data, and that of Hansen & Toong (1971*a*) and Rose & Heins (1962), agreed fairly well with a correlation of the form

$$\theta_{\text{app}} = H(C + H^{-1}(\theta_{\text{S}})),$$

† Since the value of the contact angle is calculated from an equation, it is usually referred to as 'apparent'.

where θ_S is the static advancing contact angle, C is the capillary number and H^{-1} denotes the inverse function of H (refer to figure 8). Jiang, Oh & Slattery (1978) present an explicit expression for Hoffman's correlation:

$$\frac{\cos\theta_S - \cos\theta_{app}}{\cos\theta_S + 1} = \tanh(4{\cdot}96\,C^{0{\cdot}702}).$$

They also report a rough agreement between the above and the experimental results of Schwartz & Tejada (1970). Their experiments consisted of wires composed of nylon or Teflon entering baths of various polar and non-polar liquids. Other correlations can be found in the literature (Blake & Haynes 1969; Blake & Ruschak 1979; Inverarity 1969; Schonhorn *et al.* 1966).

The interpretation of the dynamic contact angles cited above remains a subject of debate. While some claim that it represents the dynamic behaviour of the *actual* contact angle, others are a bit more cautious, referring to it as an *apparent* contact angle. The source of the controversy arises from various theoretical analyses appearing in the literature over the past decade. Hansen & Toong (1971*b*) were the first to point out the potential importance of the viscous forces even in situations of very small capillary number. They argued, with the aid of theoretical calculations, that the measured dynamic behaviour of the contact angle for a system consisting of Nujol displacing air through a Pyrex tube, could be attributed entirely to the strong influence of the viscous forces on the shape of the interface in the immediate vicinity of the moving contact line. In addition, they found that the degree to which the interface can be deformed in this region could be quite substantial. For example, their theory predicts a difference of 13° between the values of the contact angle obtained from (1) and that evaluated at a distance of $2{\cdot}6 \times 10^{-5}$ cm from the moving contact line, at a capillary number of $2{\cdot}5 \times 10^{-3}$. Other theoretical analyses using a variety of mechanisms to model the displacement process at the contact line, have also predicted a very large deformation due to the relative importance of the viscous forces (Dussan V. 1976; Huh & Mason 1977; Kafka & Dussan V. 1979; Lowndes 1980). However, this point cannot be resolved until a valid model of the region surrounding the contact line has been identified, or the shape of the interface within approximately one micrometre of the contact line has been carefully measured.

These theoretical investigations cast an additional shadow upon the usefulness of the experimentally determined correlations. They reveal that the dynamic behaviour of the measured contact angle depends to some extent on the geometry of the device in which it is measured. If this is true, then the correlations do not strictly represent material properties.

In an attempt to resolve some of these questions, and determine the source of scatter in the reported data, we have performed experiments in which silicone oil displaced air between parallel glass surfaces. This particular system was chosen because it provided a method for separating material properties from properties associated with the geometry of the system, as well as a method for determining the reproducibility of dynamic-contact-angle data. A detailed description of the experimental apparatus and preparation of the solid surfaces is given in §2. The data along with a discussion of its reproducibility, appears in §3. Implications of the data and a general discussion of the results are presented in §4.

2. Experimental techniques

Experiments on dynamic contact angles have traditionally been performed in glass capillaries because they are thought to provide a well-defined system that is convenient and reproducible. It is true that they provide a system that is extremely easy to clean and one in which the interfacial velocity may be controlled fairly precisely. Yet, the capillary is not as ideal as it first appears.

Various precision-bore capillaries, when examined under a microscope, displayed irregular, non-circular cross-sections. In addition, the inside surfaces, often assumed to be smooth, had small microscratches and larger axially directed grooves. The most significant drawback, though, is that capillaries of different size bore are necessarily manufactured under different conditions – temperature, pressure, stress fields, cooling rates, etc. Tubes of one size *may* have similar surface characteristics if they were formed under similar conditions, but it is possible, and very probable, that tubes of another size have entirely different properties. It becomes apparent, then, that tubes of dissimilar bore cannot even be considered as different batches of the same material system. As a consequence, one must be cautious when comparing data obtained from such systems if one wants to distinguish *behaviour* attributable to the material properties of the system from that due to its geometry.

Alternatively, the use of microscope slides in a parallel-plate, or slot, configuration offers the advantages of the capillary system without many of its disadvantages. The surfaces are smooth and almost optically flat, as indicated by the small number of Newton rings (5) that are usually observed between new slides. A box of slides will have been exposed to nearly identical conditions during their manufacture, and therefore, may be considered as a sample population from the collection of all slides of a particular brand, or at least, from those slides of the same lot. In contrast to the capillaries, these slides can be assembled into cells (see figure 2) with slots of various separations, while maintaining the integrity of the surface of the solid. Moreover, the fact that assembly is required allows one to select slides at random. Therefore, even if the surface properties vary slightly from slide to slide, the deviations are distributed randomly among all of the cells, and systematic error associated with non-uniform material properties is reduced.

In the system under investigation, 1000 cSt Union Carbide L-45 Silicone Oil displaced air through a slot formed by plane-parallel glass surfaces. The fluids were contained in cells composed of two Selex microscope slides separated by spacers made from 4 mil (0·01 cm) thick stainless-steel plate (shim stock), or 26 mil (0·07 cm) or 48 mil (0·12 cm) thick stainless-steel plate, as depicted in figure 2. The side and bottom edges of the slides were sealed with PTFE tape, and Plexiglas plates of $\frac{1}{4}$ in. thickness were used to distribute the load over the surfaces. The silicone oil was introduced into the cell by a positive-displacement syringe pump. The experiments were performed at $25{\cdot}0 \pm 0{\cdot}2$ °C. The density and surface tension of the silicone oil are respectively $0{\cdot}97\,\mathrm{g\,cm^{-3}}$ and $19{\cdot}7\,\mathrm{dyn\,cm^{-1}}$.

The method of pretreating the slides was adapted from a method used to prepare slides for vapour deposition of metals. Instead of treating single slides, a set of slides was treated as a batch, so that they would be exposed to an identical environment. Two sets were placed through the procedure in parallel. From a box containing 72 slides, 30 slides were selected at random, and placed in a polypropylene slide staining rack.

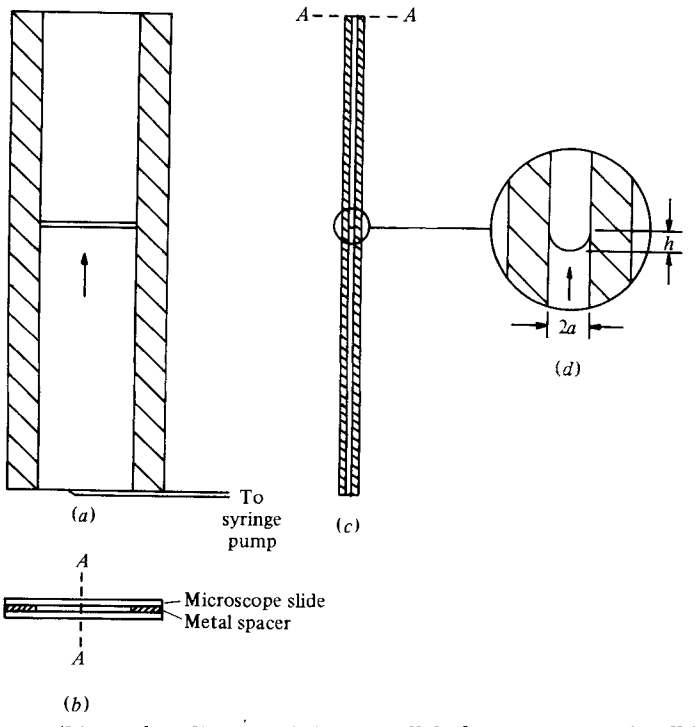

FIGURE 2. Silicone oil is used to displace air in a parallel-plate geometry. A cell is constructed of two glass microscope slides separated by metal spacers. Cells having different slot widths can then be assembled by using spacers of different thicknesses. The elevation (*a*) is the perspective seen by the camera. The interface appears as a horizontal band. The plan view is shown in (*b*), with (*c*) giving section *A*–*A*. This is the perspective one might have if the interface could be observed at the centre of the slot if the spacer were not there. An exploded view of the interface in this view is given in (*d*).

From another box of the same lot 30 additional slides were selected and placed on a second rack. The racks were then immersed in 500 ml of rapidly boiling distilled, deionized water for 30 min, after which about 50 ml of the liquid was drained off the top. Make-up water was added to maintain the liquid level. The premise is that any material on the surface of the glass will partition itself between the surface phase and the bulk liquid, or in the case of surface-active contaminants, be removed by the rising bubbles and carried to the surface of the liquid, and subsequently drained off. The slides were submerged in four more baths, removed, and placed on polyethylene slide holders, and dried in an oven at 60 °C for two hours. The staining racks were boiled in ten baths of distilled, deionized water for 30 min each prior to their first contact with the slides. The slide holders were baked at 60 °C for 120 hours. These precautions were taken in order to remove free monomer, plasticizer, or other additives that might have been present in the plastic.

The slot thickness was determined by locating the inside surfaces of the slides through a microscope. Because the slides were transparent and essentially free from surface defects, it was necessary to mark a portion of the surfaces in order to locate them accurately once the cell was assembled. The parts of the surfaces so altered never came in contact with the advancing fluid. The value of the slot thickness used in calculations

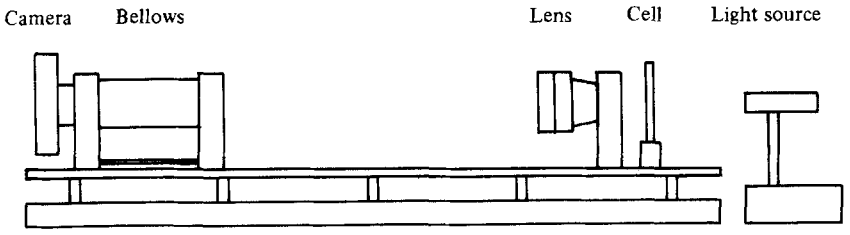

FIGURE 3. The image-recording system consists of a 35 mm camera with motor drive, bellows, 24–48 mm zoom lens, microscope light source, and optical rail on a granite table.

of the contact angle from any particular cell represented the average of several measurements at the centre line and near each edge, in the region that had been marked before assembly. Tests had indicated that the uncertainty in the value obtained at any particular point was about two micrometres, and that the standard deviation of the mean centre-line thickness was 3–4 μm.

The movement of the interface was observed through and recorded by an optical system as depicted in figure 3. The relative placement of the subject, lens and camera, and the focal length of the lens determine the magnification that one attains. In order to obtain a range of magnifications for fixed lens and camera locations, a wide-angle zoom lens was used in the reversed position. A 35 mm camera was equipped with a motor drive so that images could be obtained at rates of almost 4 frames per second. All components were mounted on an optical bench atop a granite table to provide stability. The images were recorded on a fine-grain panchromatic film and developed in a diluted developer for lower grain and higher resolution. Optical distortion, checked by photographing a stage micrometer, was found to be negligible in the field of view for all magnifications used. The stage micrometer was also used to provide the length scale for determining actual magnifications from the photographs.

When backlit, and observed from the perspective depicted in figure 2(*a*), the interfaces appeared as dark bands on a bright field. These bands were horizontal in the field of view, indicating that edge effects due to the spacers were negligible, and that the plates were parallel. For the silicone-oil–air–glass system, the top side of a band is the contact line, while the bottom side is the apex of the meniscus; hence an apex height h can readily be calculated by measuring the height of the band. It is one of only a few characteristics of the interface shape capable of being measured, and perhaps the only one obtainable from a slot geometry. Note that the shape of the interface, as depicted in figure 2(*b*), is not experimentally observable. Consequently, if one wishes to characterize the interface shape by a contact angle, one must calculate an apparent contact angle from the apex height and the average slot thickness through (1). This equation gives the angle that would exist if the interface was a segment of a circular cylinder. In capillaries, interfaces moving at speeds reported here were observed to resemble spherical caps. Comparisons of enlarged photographs of such interfaces with circles showed that they were virtually identical, thus justifying the use of (1). However, one must always keep in mind that, in the data reported in § 3, the apparent contact angle and the dimensionless apex height h/a are equivalent.

The other quantity obtained from the photograph images was the velocity of the contact line. Velocities were calculated from the change in the location of the contact

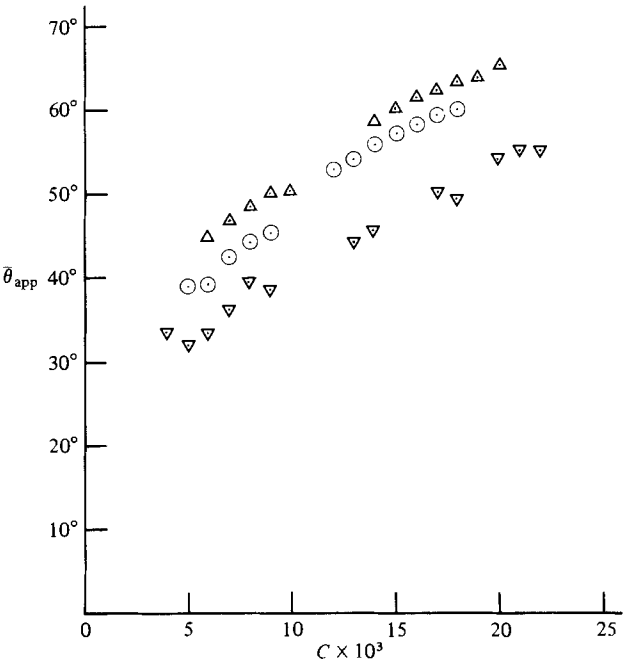

FIGURE 4. Variation of the mean apparent contact angle, $\bar{\theta}_{app}$, with capillary number during the displacement of air by silicone oil in between plane-parallel glass surfaces of nominal separation 0·01 cm (▽), 0·07 cm (○) and 0·12 cm (△), at 25·0 ± 0·2 °C. The oil has a viscosity μ of 970 cP and a surface tension σ of 19·7 dyn cm^{-1}. (U = 2·03 C cm s^{-1}.)

line in successive frames, knowing the time interval between frames. The experiments were designed to be conducted at constant velocity. In the 0·07 cm slots, and more so in the 0·12 cm slots, periodic oscillations of the velocity and apparent contact angle were observed. These oscillations were attributed to the syringe pump and are currently being investigated.

3. Experimental results

The two measured quantities, the apex height and the change in contact-line location per unit time, were converted to the dimensionless quantities: the apparent contact angle θ_{app} and the capillary number C. The capillary number can be viewed as a dimensionless velocity, defined as $\mu U/\sigma$, where U denotes the speed of the contact line, μ the viscosity of the advancing fluid, and σ the surface tension of the fluid–fluid interface. The data could then be presented in several ways, each illustrating slightly different, but equally important ideas.

The overall trends became apparent upon examining the summary of the data given in figure 4.† Each point represents the average of at least five measurements of the apparent contact angle in one size slot, within an interval given by ± 0·0005 of the value of C indicated. These points represent 794 measurements obtained from 26 of

† By placing a drop of oil on a horizontal glass slide, it was concluded that the static contact angle has a value of less than 1°. However, no attempt was made to measure its value within the cells at very slow speeds because of the inaccuracy of this method in measuring small contact angles.

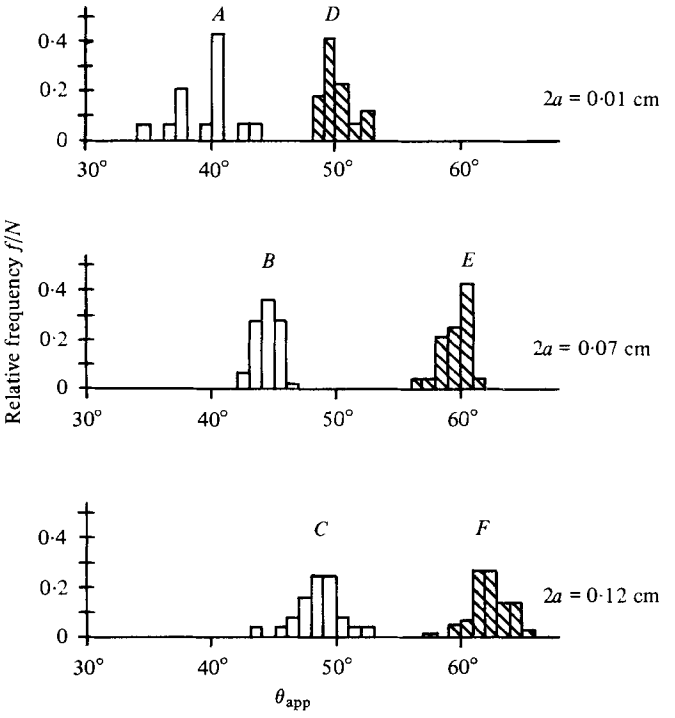

FIGURE 5. Conditional distributions of the apparent contact angle at capillary numbers of $C = 0{\cdot}008 \pm 0{\cdot}0005$ (unshaded histograms) and $C = 0{\cdot}017 \pm 0{\cdot}0005$ (shaded histograms). The mean apparent contact angle $\bar{\theta}_{app}$, standard deviation s, and sample size N for each distribution are given in the following table.

	$\bar{\theta}_{app}$	s	N
A	39·42	2·29	14
B	44·46	0·90	36
C	48·54	1·86	24
D	50·12	1·13	17
E	59·62	1·15	24
F	62·39	1·55	56

the 30 cells, 8 of the 0·01 cm separation, and 9 each of the 0·07 and 0·12 cm separations. Of these measurements, 36 fell into intervals containing four points or less, with the remainder distributed with an average of 20 measurements per interval. Of the four remaining cells, one had surfaces that were not parallel, another could not be calibrated owing to overexposure of the calibration frames, and the last two were cracked during assembly. The curves in figure 4 show two important trends. The apparent contact angle is a monotonic non-decreasing function of the speed of the contact line, a behaviour characteristic of all reported data in the literature. Moreover, the dynamic behaviour of the apparent contact angle depends upon the *size* of the slot from which the measurements were obtained.

This last point is illustrated more clearly in figure 5, where the spread in the values of the apparent contact angle at two specific contact-line speeds is displayed. The feature to note is that even though the apparent contact angles vary about their means with a standard deviation of 1–2°, the sample distribution obtained form the 0·01 cm slot is

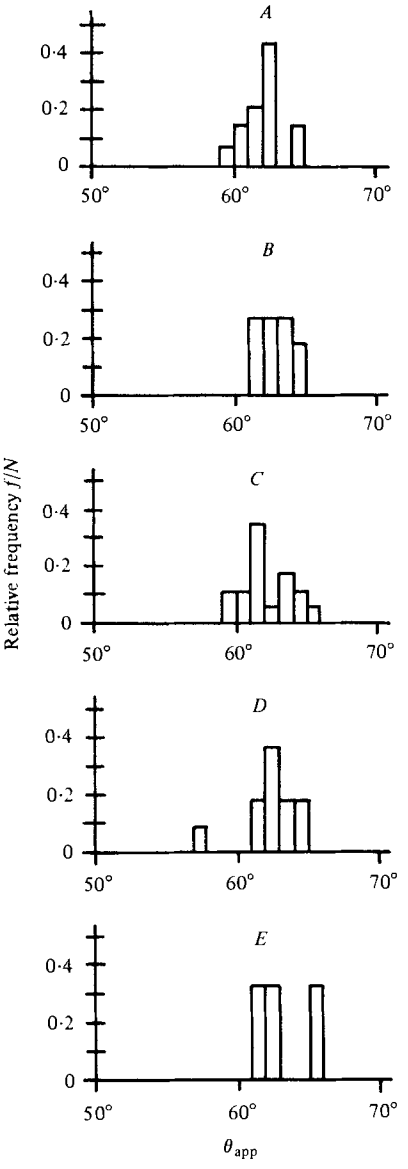

FIGURE 6. Variation of the mean apparent contact angle from cell to cell, and the variation of the apparent contact angle within any given cell for a separation of 0·12 cm at a capillary number of $C = 0{\cdot}017 \pm 0{\cdot}0005$. The mean apparent contact angle $\overline{\theta}_{app}$, standard deviation s, and sample size N for each distribution are given in the following table.

	$\overline{\theta}_{app}$	s	N	$2a$
A	62·15	1·21	14	0·1214
B	62·93	0·97	11	0·1215
C	62·12	1·79	17	0·1215
D	62·37	1·89	11	0·1209
E	63·24	2·21	3	0·1208

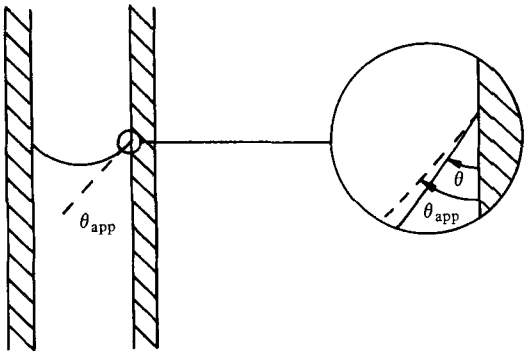

FIGURE 7. Conceptualization of the deformation of the interface in a region near the contact line owing to the relative importance of viscous forces.

virtually distinct from that obtained from the 0·12 cm slot. Indeed, this implies that there is a significant difference between the population mean apparent contact angles for these two size slots. One must keep in mind that increasing the number of measurements and the number of cells would narrow the distributions even further.

In order to investigate the sensitivity of the apparent contact angle to the state of the glass surface, all of the data used to calculate one specific point in figure 4 were examined in detail. The point corresponding to a capillary number of 0·017 for the 0·12 cm slot was chosen because this data comes from five different cells, a relatively high number when compared with the other points. Histograms are presented in figure 6 for each of these cells. Note that the variation of the mean value of the apparent contact angle from cell to cell is about 0·5°, while the standard deviation within each cell lies between 1 and 2°. Since the mean from cell to cell varied very little, and since the standard deviations were nearly the same, one can conclude that the nature of the surface was the same for all the microscope slides.

4. Interpretation of data and discussion of results

Various conclusions can be drawn from the experimental data presented in figure 4. The most obvious is that the contact angle, even though it is measured at small capillary numbers, does not represent the *actual* contact angle. Since the actual contact angle is a material property of the system, it cannot depend on the geometry of the apparatus in which it is measured. However, it is fairly clear that the angle reported in figure 4 does depend on the width of the slot; hence it cannot be the actual contact angle.

It is not uncommon to find in the literature dynamic contact angles measured in a similar fashion referred to as actual contact angles. This interpretation is understandable. As reported in §2, upon photographing air–oil meniscii moving through 0·2 cm inner diameter glass tubes at the same capillary numbers as those that appear in figure 4, we found no distinction between them and arcs of circles, even in the region very close to the moving contact line. Measuring the contact angle by means of a protractor or by using (1) gave the same value to within experimental accuracy. Thus, based solely upon observations of individual meniscii, there is a strong temptation to refer to this angle as the actual contact angle.

On the other hand, our conclusion that this angle cannot be the actual contact angle

is consistent with many theoretical analyses that have appeared in the literature over the last decade. As discussed in § 1, these studies indicate that the fluid interface can undergo significant deformation in the region very close to the moving contact line owing to the relative importance of the viscous forces. It is this effect that causes θ_{app} to differ in value from θ. Even though it can occur at values of the capillary number much less than one, these studies have the common characteristic that $\theta_{app} \to \theta$ as $C \to 0$ (this limit need not correspond to $U \equiv 0$). An illustration of this is given in figure 7. However, in some of these theoretical studies where data from the literature is used as supporting evidence, the authors make unnecessary assumptions to justify their contentions. For example, Huh & Mason (1977) and Lowndes (1980) compare experimentally measured values of θ_{app} for immiscible-fluid displacement through a capillary with that calculated from their analyses after the following assumptions have been made: (i) a specific model by which the liquid is allowed to slip on the surface of the solid near the moving contact line is assumed; in addition, a specific value for the slip length (10^{-7} cm) must be specified; and (ii) the value of the actual contact angle is assumed not to depend on the speed of the contact line. For capillary numbers less than 7×10^{-2} they find that some angles agree to within 2°, others to within 12°. In contrast, we are able to draw our conclusion from the data presented in § 3 independent of any such assumptions.

Another important conclusion that can be drawn from the data presented in figure 4 is that the usual hydrodynamic-modelling assumptions are insufficient for describing the motion of fluids containing moving contact lines. Again this follows directly from the fact that the dynamic variation of the apparent contact angle, i.e. the quantity h/a, depends on the width of the slot.

In order to demonstrate the above, it is necessary first to identify the parameters that would describe completely the motion of the fluids assuming that the usual hydrodynamic model is valid. Using the gap width $2a$ of the slot as the characteristic length scale, the speed U of the contact line as the velocity scale, and σ/a as the scale of the stress, the Navier–Stokes equation for an incompressible fluid introduces the Reynolds number $R = Ua\rho/\mu$, and the Bond number $B = g\rho a^2/\sigma$. The boundary condition at the fluid–fluid interface introduces the capillary number $U\mu/\sigma$ and the viscosity ratio μ_A/μ_R, the subscripts A and R denoting respectively the advancing and receding fluids. As with static systems the value of the contact angle θ must also be given, the only difference being that its value may depend on some dynamical aspect of the system such as the spread of the contact line, $\theta(U)$. This is the same angle previously referred to as the *actual* contact angle. In general, it would be anticipated that $\theta(U)$ depends directly on the nature of the two immiscible fluids and surface of the solid, thus changing for different material systems.† Therefore, if an analysis was performed on the motion of the fluids, an expression of the following form would be derived:

$$\frac{h}{a} = f(R_A, B_A C_A, \mu_A/\mu_R, \theta(U)). \tag{2}$$

The experiments that produced figure 4 were performed at restricted values of the above parameters. Since the Bond number was always less than 0·18, it may be con-

† This justifies leaving the variables upon which θ depends in dimensional form.

cluded that gravity had a negligible effect on the shape of the fluid interface.† Hence, the dependence of h/a on B_A may be deleted. The value of the Reynolds number was always small, lying within the interval $[10^{-6}, 10^{-3}]$. Hence, it may also be deleted from (2). Finally, the viscosity ratio must be considered a constant, since the same fluids were used in all the experiments. Therefore, it can be concluded that if the usual hydrodynamic-modelling assumptions are appropriate for these experiments, then the variation of h/a, and hence θ_{app}, can only come from C_A or $\theta(U)$. Thus, the dependence of θ_{app} on the gap width $2a$ must imply that this model is insufficient to describe the motion of fluids containing moving contact lines.

This conclusion is consistent with theoretical investigations. It has been found that a singularity always appears in the analysis if the usual hydrodynamic modelling assumptions are made (see Dussan V. (1979) for a critical review of the literature). In brief, this singularity appears in the stress tensor as an infinite drag on the solid, in the energy equation as an infinite rate of dissipation, and at the contact line in the equation that describes the shape of the interface. Its appearance in this latter equation is of such a form that the contact-angle boundary condition cannot be used. In order to avoid this singularity, there have been various theoretical analyses which have used models that have differed from the usual one (Hocking 1977; Huh & Mason 1977; Dussan V. 1976; Greenspan 1978), all of which involve introducing a boundary condition which allows the fluids to slip along the wall. All of these analyses have the characteristic that only within a small region in the immediate vicinity of the moving contact line does the fluid slip substantially along the wall. It is tempting to conclude that the size of this region is related to the length scale missing from the above dimensional analysis of our data. The fact that these theories predict shapes of the fluid interface consistent with that depicted in figure 7 – i.e. the interface has a constant curvature except in the region very close to the moving contact line – is encouraging; however, more careful experimental observations are needed before any definite association can be made.

We were able to find data in the literature with a behaviour similar to that illustrated in figure 4. The data were obtained from observation of the unsteady spreading of very small drops of polymer on horizontal metal surfaces (Schonhorn *et al.* 1966). Since our analysis of the data is quite different from these authors, and our conclusions run directly counter to theirs, we have delayed discussing it until this point. They found that all of their data could be represented by single curves when plotted as $r(t)/r_0$ versus $\sigma t/\mu L_w$ or $\cos\theta_{app}(t)/\cos\theta_\infty$ versus $\sigma t/\mu L_w$. Here $r(t)$ denotes the instantaneous radius of the wetted area, and r_0 is the value of the radius when the instantaneous apparent contact angle $\theta_{app}(t)$ is 90°. The limiting static contact angle is denoted by θ_∞ and time is represented by t. L_w is an empirically determined adjustable parameter having units of length, which Schonhorn *et al.* have found to be dependent only on the polymer and metal solid used. Since the parameter $\sigma t/\mu L_w$ is independent of the size of the drops, they conclude that the kinetics of wetting is independent of the size of the drop. However, these plots already have an implicit dependence on the geometry of the meniscus. In order to eliminate this, we used their data to calculate θ_{app} versus C. When this is done, something quite different is revealed. In figure 8, we have plotted the data obtained from the spreading of two different size drops of Elvax 220† on aluminium at

† This conclusion is based on the results of a detailed asymptotic analysis of the affect of gravity on the shape of the static meniscus in the limit as $B \to 0$. Specifically, (1) predicts the static contact angle to within 0·6° for a contact angle of 45°.

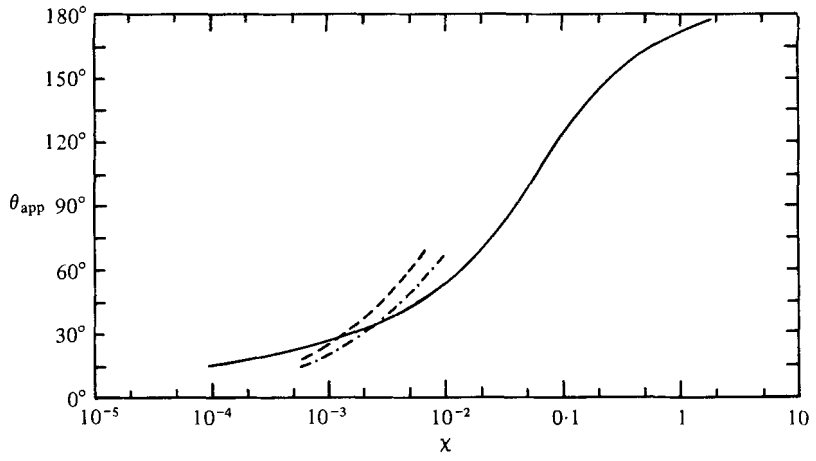

FIGURE 8. Variation of the apparent contact angle with velocity. Hoffman's correlation $H(\chi)$ is denoted by the solid line (——), with $\chi = C + H^{-1}(\theta_s)$, where C is the capillary number and θ_s is the static advancing contact angle. The data obtained from Schonhorn *et al.* (1966) for the spreading of drops, rearranged into an appropriate form, are denoted by the broken lines. A 0·0055 g polymer drop is represented by the dashed line (– – – –), and a 0·0200 g drop is represented by the dot-dashed line (–.–.–). For these curves $\chi = C$.

170 °C. One can see that indeed the rate of spreading does depend on the size of the drops. As the drop of mass 0·0055 g spreads out, the radius of the contact line varies roughly from 0·14 to 0·28 cm, while the radius of the drop of mass 0·020 g varies from 0·23 to 0·46 cm. It is interesting to note that the relatively small size ratios of 3 : 2 could cause differences in apparent contact angle of 10°. Since the reported viscosity of the fluid is 2000 P, this may in fact be caused by non-Newtonian affects.

We would like to acknowledge the efforts of Joseph Vadapalas, who provided the initial experimental design; Pamela Jackson, who designed and built an optical system upon which the one we used is based; and Fred Kafka, whose many efforts were invaluable to the initial development of the study. We would also like to acknowledge Union Carbide for their generous samples of silicone oil.

This work was made possible by the support of a grant from the National Science Foundation, Fluid Mechanics Program.

REFERENCES

BLAKE, T. D. & HAYNES, J. M. 1969 Kinetics of liquid/liquid displacement. *J. Colloid Interface Sci.* **30**, 421.

BLAKE, T. D. & RUSCHAK, K. J. 1979 A maximum speed of wetting. *Nature* **282**, 489.

DUSSAN, V., E. B. 1976 The moving contact line: the slip boundary condition. *J. Fluid Mech.* **77**, 665.

DUSSAN, V., E. B. 1979 On the spreading of liquids on solid surfaces: static and dynamic contact lines. *Ann. Rev. Fluid Mech.* **11**, 371.

GREENSPAN, H. P. 1978 On the motion of a small viscous droplet that wets a surface. *J. Fluid Mech.* **84**, 125.

† Elvax 200 is an ethylene-vinyl-acetate copolymer developed by DuPont.

HANSEN, R. J. & TOONG, T. Y. 1971*a* Interface behavior as one fluid completely displaces another from a small-diameter tube. *J. Colloid Interface Sci.* **36**, 410.

HANSEN, R. J. & TOONG, T. Y. 1971*b* Dynamic contact angle and its relationship to forces of hydrodynamic origin. *J. Colloid Interface Sci.* **37**, 196.

HOCKING, L. M. 1977 A moving fluid interface. Part 2. The removal of the force singularity by a slip flow. *J. Fluid Mech.* **79**, 209.

HOFFMAN, R. 1975 A study of the advancing interface. I. Interface shape in liquid–gas systems. *J. Colloid Interface Sci.* **50**, 228.

HUH, C. & MASON, S. G. 1977 The steady movement of a liquid meniscus in a capillary tube. *J. Fluid Mech.* **81**, 401.

INVERARITY, G. 1969 Dynamic wetting of glass fibre and polymer fibre. *Brit. Polymer J.* **1**, 245.

JIANG, T.-S., OH, S.-G. & SLATTERY, J. C. 1979 Correlation for dynamic contact angle. *J. Colloid Interface Sci.* **69**, 74.

KAFKA, F. Y. & DUSSAN, V., E. B. 1979 On the interpretation of dynamic contact angle in capillaries. *J. Fluid Mech.* **95**, 539.

LOWNDES, J. 1980 The numerical simulation of the steady movement of a fluid meniscus in a capillary tube. *J. Fluid Mech.* **101**, 631.

ROSE, W. & HEINS, R. W. 1962 Moving interfaces and contact angle rate-dependence. *J. Colloid Interface Sci.* **17**, 39.

SCHONHORN, H., FRISCH, H. L. & KWEI, T. K. 1966 Kinetics of wetting of surfaces by polymer melts. *J. Appl. Phys.* **37**, 4967.

SCHWARTZ, A. M. & TEJADA, S. B. 1972 Studies of dynamic contact angles on solids. *J. Colloid Interface Sci.* **38**, 359.

SCHWARTZ, A. M. & TEJADA, S. B. 1970 *N.A.S.A. Contract Rep.* CR 7278.